Biochimica et Biophysica Acta, 680 (1982) 343–351
Elsevier Biomedical Press

BBA 41072

A DEMONSTRATION OF THE PHYSIOLOGICAL ROLE OF MEMBRANE PHOSPHORYLATION IN CHLOROPLASTS, USING THE BIPARTITE AND TRIPARTITE MODELS OF PHOTOSYNTHESIS

PHILIP HAWORTH, DAVID J. KYLE and CHARLES J. ARNTZEN

MSU-DOE Plant Research Laboratory, Michigan State University, East Lansing, MI 48824 (U.S.A.)

(Received August 31st, 1981)
(Revised manuscript received January 4th, 1982)

Key words: Membrane phosphorylation; Electron transfer; Energy transduction; Light-harvesting complex; Photosystem II; (Chloroplast membrane)

Using the equations derived from the bipartite and tripartite models for photosynthetic organization in green plants, we have been able to characterize the effect of membrane phosphorylation on energy transduction. Phosphorylation reversibly increases α (the proportion of absorbed quanta going directly to Photosystem (PS) I). This increase in α we believe to be due to a decrease in the coupling between the PS II core and its associated light-harvesting complex [$\Psi T(3,2)\cdot\Psi T(2,3)$]. Phosphorylation also reversibly increases the transfer of energy from PS II to PS I [$\psi T_{(II\rightarrow I)}$]. We propose that membrane phosphorylation provides the in vivo control of α, $\Psi T(3,2)\cdot\Psi T(2,3)$ and $\psi T_{(II\rightarrow I)}$. From the data we present it is clear that the changes caused in energy distribution as a result of phosphorylation are large enough to induce real changes in electron-transfer reactions. The effects of phosphorylation on these parameters are distinct from those of Mg^{2+} depletion. We have discussed changes in $\Psi T(3,2)\cdot\Psi T(2,3)$ (the coupling term) with respect to the 'connected package' model of photosynthetic units (Butler, W.L. (1980) Proc. Natl. Acad. Sci. U.S.A. 77, 4697–4701) and the proposed α- and β-centers of PS II (Melis, A. and Homann, P.H. (1976) Photochem. Photobiol. 23, 345–350). The demonstration of changes in reversible coupling [$\Psi T(3,2)\cdot\Psi T(2,3)$] strongly supports a connected package model in which the degree of 'connectivity' is under physiological control.

Introduction

The adaptive changes in light-harvesting properties of photosynthetic membranes referred to as State 1-State 2 transitions exist to maintain a balance in noncyclic electron flow through the two photosystems [1–5]. The biochemical/biophysical events involved in the State 1-State 2 transition have been equated extensively with cation-induced effects on energy distribution in thylakoids [6–8]. Cation-regulated energy distribution between PS I and PS II has been monitored via chlorophyll fluorescence changes, alterations in the quantum yield of partial reactions, and directly measured changes in *P*-700 photooxidation and electron transfer [6–9]. The nature of these cation effects have been rigorously defined and quantified by Butler and co-workers in the tripartite [10–12] and bipartite models [13] of pigment organization.

The data of Steinback et al. [14,15] have clearly shown that the cation-induced changes in energy-distribution process are dependent on a surface-exposed portion of the light-harvesting complex [16] serving PS II (LHC_{II}). The observation that in

Abbreviations: PS, photosystem; LHC_{II}, light-harvesting complex of PS II; Chl, chlorophyll; Tricine, *N*-tris(hydroxymethyl)methylglycine.

vitro phosphorylation [17–19] of this exposed segment causes a redistribution of absorbed quanta, similar to State 1-State 2 transitions, has provided a new avenue to investigate the physiological mechanism of the transitions [20]. Data have been presented [5] to formulate a model in which the phosphorylation of LHC_{II} is linked to the oxidoreduction state of the electron-transport chain. The existence of this control proces leads us to believe that phosphorylation of LHC_{II} is the in vivo control for State 1-State 2 transitions.

In this work we will demonstrate, using low-temperature (77 K) fluorescence induction transients, and the models and equations of Butler and co-workers [10–13] that phosphorylation simultaneously reduces LHC_{II}-PS II coupling and increases exciton transfer from PS II to PS I.

Materials and Methods

Chloroplast membrane preparations were as described by Kyle et al. [21]. Three types of membrane samples were used in these studies. Samples were placed in a glass water bath for 5 min to reach room temperature, and ATP was added to a concentration of 200 μM. Phosphorylated membranes are defined as those incubated for 15 min light followed by 15 min dark in the presence of NaF, dephosphorylated samples by 15 min light followed by 15 min dark before addition of NaF. Nonphosphorylated samples spent the full 30 min in the dark before adding NaF. Fluorescence induction curves were measured using the apparatus shown in Fig. 1. Fluorescence from PS I was measured using a 735 nm narrow band pass filter (band pass $\pm$ 2.5 nm at 50% T_{max}, T_{max} at 735 nm = 45%). PS II fluorescence was measured using a 695 nm band pass filter (band pass $\pm$ 4 nm at 50% T_{max}, T_{max} at 695 nm = 17%). The emission from LHC_{II} was measured at 684 nm (band pass $\pm$ 4.5 nm at 50% T_{max}, T_{max} at 684 nm = 52%). Induction curves were measured in 1 cm^2 disposable 3-ml plastic cuvettes using 200 μl of sample ([Chl] = 25 μg/ml). Sample buffer contained 10 mM Tricine-NaOH (pH 7.8), 10 mM NaF and 30% glycerol $\pm$ 5 mM $MgCl_2$. Samples were frozen uniformly by partial immersion of the cuvettes in liquid nitrogen and the sample was kept frozen during measurement of the induction transient by flooding the frozen sample with liquid nitrogen. Excitation of fluorescence was achieved using blue light (Corning filter No. 4-96) with an intensity of 100 W/m^2.

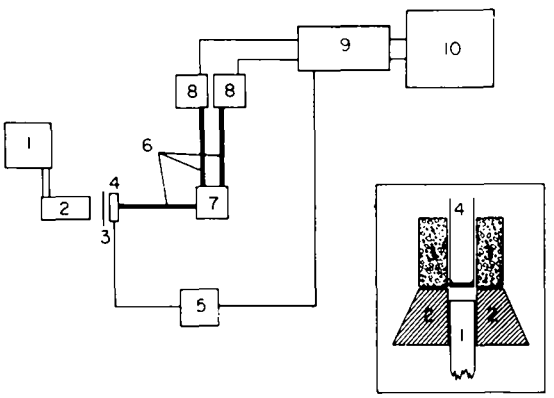

Fig. 1. Apparatus for determination of low-temperature fluorescence induction transients: (1) d.c. power supply, (2) light source, (3) blue filter (Corning No. 4-96), (4) automatic shutter, (5) shutter control and oscilloscope trigger, (6) trifurcated light pipe, (7) sample holder (see inset), (8) photodiode with narrow band pass filter, (9) recording oscilloscope, (10) x-y chart recorder. (Inset) Sample holder: (1) trifurcated light pipe, (2) rubber stopper for insulation and mounting, (3) cell holders, (4) disposable plastic cuvette.

Results

Low-temperature (77 K) fluorescence induction curves at 695 nm are presented in Fig. 2. The data show a clear difference of $MgCl_2$ effects on the extent of $F_v (F_v = F_m - F_0)$ in nonphosphorylated and phosphorylated membranes. A low value of F_v^{695} reflects a high energy transfer from PS II to PS I, while a high value reflects a low energy transfer [13]. The full fluorescence induction data at 695 and 735 nm for nonphosphorylated, phosphorylated and dephosphorylated thylakoid membranes are summarized in Table I. We have applied the equations for the bipartite model derived by Butler and Kitajima [13] to the data presented in Table I to calculate values of α (the proportion of absorbed quanta going directly to PS I) and $\psi T_{(II \rightarrow I)(m)}$ (the total maximum energy transfer from PS II to PS I). These data are summarized in Table II; examples of the calculations are presented elsewhere [13,22]. The values of α and $\psi T_{(II \rightarrow I)(m)}$ calculated for nonphosphorylated membranes

TABLE I

LOW-TEMPERATURE FLUORESCENCE INDUCTION DATA AT 695 AND 735 nm IN NONPHOSPHORYLATED, PHOSPHORYLATED AND DEPHOSPHORYLATED THYLAKOID MEMBRANES

Data are presented as mean ± S.E., sample size = 5. [Chl] per sample = 25 μg/ml; sample volume = 200 μl.

	Nonphosphorylated			Phosphorylated			Dephosphorylated		
	F_0^{695}	F_m^{695}	F_v^{695}/F_m^{695}	F_0^{695}	F_m^{695}	F_v^{695}/F_m^{695}	F_0^{695}	F_m^{695}	F_v^{695}/F_m^{695}
$+MgCl_2$ (5 mM)	174 ± 12	454 ± 13	0.62	136 ± 1	266 ± 1	0.49	133 ± 3	300 ± 22	0.56
$-MgCl_2$	149 ± 1	289 ± 2	0.48	128 ± 3	216 ± 5	0.41	120 ± 4	227 ± 11	0.47
	F_0^{735}	F_m^{735}		F_0^{735}	F_m^{735}		F_0^{735}	F_m^{735}	
$+MgCl_2$ (5 mM)	378 ± 12	483 ± 15		435 ± 12	548 ± 15		364 ± 21	453 ± 27	
$-MgCl_2$	516 ± 9	632 ± 6		487 ± 7	586 ± 9		451 ± 13	563 ± 15	

TABLE II

CALCULATED VALUES OF α AND $\psi T_{(II \rightarrow I)(m)}$ IN THE PRESENCE AND ABSENCE OF $MgCl_2$ USING THE BIPARTITE EQUATIONS OF BUTLER AND KITAJIMA [13] AND THE DATA OF TABLE I

	Nonphosphorylated	Phosphorylated	Dephosphorylated
α $+MgCl_2$	0.23	0.34	0.23
α $-MgCl_2$	0.29	0.33	0.26
$\psi T^{-}_{(II \rightarrow I)(m)}$	0.16	0.27	0.16
$\psi T^{-}_{(II \rightarrow I)(m)}$	0.25	0.34	0.25

show the response to Mg^{2+} described by Butler and co-workers [13,22]. Phosphorylation of the membranes [21] caused α and $\psi T_{(II \rightarrow I)(m)}$ to increase in relation to the nonphosphorylated membranes. The value of $\psi T_{(II \rightarrow I)(m)}$ for phosphorylated membranes still shows an Mg^{2+} effect, $\psi T^{-}_{(II \rightarrow I)(m)}$ is slightly higher than $\psi T^{+}_{(II \rightarrow I)(m)}$, but α values appear unaffected by change in Mg^{2+} level. Dephosphorylation of the membranes caused values of α and $\psi T_{(II \rightarrow I)(m)}$ to return to those of the nonphosphorylated membranes and also regenerated the full Mg^{2+} effect.

Apart from energy transfer between the two photosystems a second factor in energy distribution is the coupling between LHC_{II} and PS II. It is possible to calculate a value for this coupling ($\Psi T(3,2) \cdot \Psi T(2,3)$) using the tripartite model of the pigment bed [10–12]. For these calculations it is necessary to determine fluorescence induction curves at 695 and 684 nm. These data are summarized in Table III. The calculation of $\Psi T(3,2) \cdot \Psi T(2,3)$ involves three steps as described in Ref. 11. We have assumed values of some parameters from this reference.

$$\frac{F^{684}\gamma}{F_m^{684}} = \frac{\gamma(1 - \Psi T(3,2) \cdot \psi T(2,3)_{(m)})}{\gamma + \beta \psi T(2,3)_{(m)}} \quad (1)$$

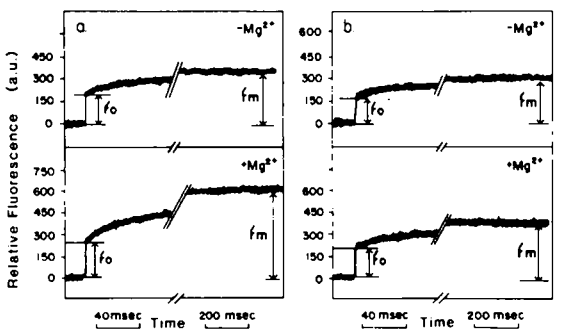

Fig. 2. Low-temperature (77 K) fluorescence induction transients at 695 nm for (a) nonphosphorylated membranes ± $MgCl_2$ and (b) phosphorylated membranes ± $MgCl_2$. a.u., arbitrary units.

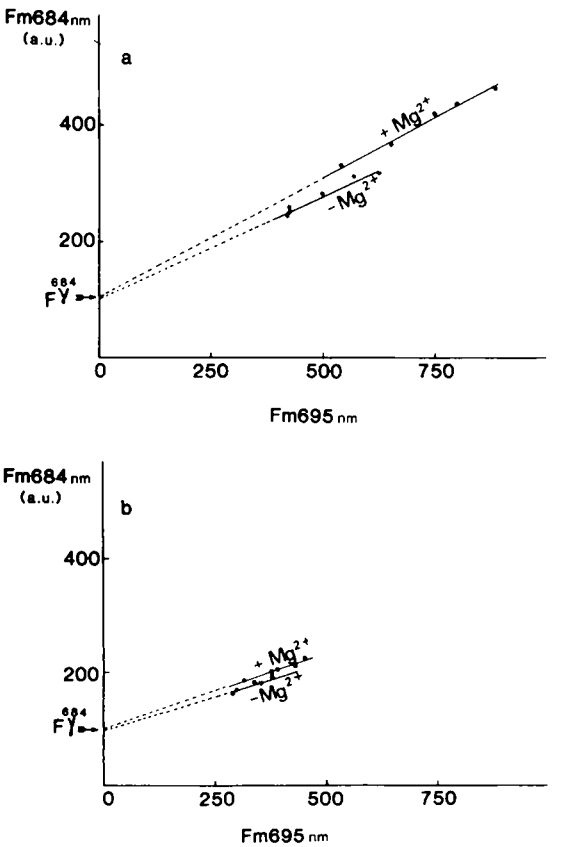

Fig. 3. Plots of F_m^{684} vs. F_m^{695} at 77 K for (a) nonphosphorylated membranes and (b) phosphorylated membanes. a.u., arbitrary units.

TABLE III

LOW-TEMPERATURE FLUORESCENCE INDUCTION DATA AT 695 AND 684 nm IN NONPHOSPHORYLATED, PHOSPHORYLATED AND DEPHOSPHORYLATED THYLAKOID MEMBRANES

Data are presented as mean ± S.E., sample size = 5. [Chl] per sample = 25 μg/ml; sample volume = 200 μl.

	Nonphosphorylated			Phosphorylated			Dephosphorylated		
	F_0^{695}	F_m^{695}	F_v^{695}/F_m^{695}	F_0^{695}	F_m^{695}	F_v^{695}/F_m^{695}	F_0^{695}	F_m^{695}	F_v^{695}/F_m^{695}
$+MgCl_2$ (5 mM)	299 ± 18	695 ± 43	0.66	192 ± 10	388 ± 19	0.50	195 ± 10	468 ± 15	0.58
$-MgCl_2$	196 ± 2	424 ± 2	0.44	169 ± 6	329 ± 13	0.38	153 ± 6	354 ± 15	0.45
	F_0^{684}	F_m^{684}		F_0^{684}	F_m^{684}		F_0^{684}	F_0^{684}	
$+MgCl_2$ (5 mM)	157 ± 11	392 ± 24		105 ± 5	201 ± 6		160 ± 5	304 ± 8	
$-MgCl_2$	117 ± 1	247 ± 6		94 ± 4	176 ± 6		146 ± 4	247 ± 8	

The value for γ (the fraction of absorbed quanta going directly to LHC_{II} is taken as 0.5, β as 0.2 and $\psi T(2,3)_{(m)}$ as 0.90; a description of these values can be found elsewhere [11]. The value of $F^{684}\gamma$ can be calculated from the plot of F_m^{684} against F_m^{695} (at 77 K), as shown in Fig. 3. In this figure we present the plots for both nonphosphorylated membranes (Fig. 3a) and phosphorylated membranes (Fig. 3b). Although the slope of these lines is different in each case, identical values of $F^{684}\gamma = 100$ were determined. Using $F^{684}\gamma = 100$, a value of $\Psi T(3,2) \cdot \psi T(2,3)_{(m)}$ can be calculated from Eqn. 1 and substituted into Eqn. 2:

$$\frac{F_v^{695}}{F_m^{695}} = \frac{\Psi TII \cdot \Psi tII}{1 - \Psi T(3,2) \cdot \psi T(2,3)_{(m)}(1 - \Psi TII \cdot \Psi tII)} \quad (2)$$

$\Psi TII \cdot \Psi tII$ is a measure of the efficiency of coupling between the PS II core antenna (Chl a_{II}) and the PS II reaction center. The value of $\Psi TII \cdot \Psi tII$ calculated from this equation is used in Eqn. 3 to calculate $\Psi T(3,2) \cdot \Psi T(2,3)$:

$$\frac{F_v^{695}}{F_m^{695}} = \frac{\Psi TII \cdot \Psi tII}{1 - \Psi T(3,2) \cdot \Psi T(2,3)} \quad (3)$$

Our results from these determinations are presented in Table IV. In nonphosphorylated membranes we observed a decrease in the coupling between LHC_{II} and PS II (components 3 and 2, respectively [10]) when the membranes are depleted of Mg^{2+}. Phosphorylation of the membranes produces a much larger decrease in this coupling: in addition, no Mg^{2+}-induced decrease was observed. Dephosphorylation of the membranes reversed this trend.

Discussion

The tripartite and bipartite models were developed to describe the in vivo pigment organization in green plants [10–13,26]. The tripartite model assumes three major pigment-protein assemblies which are in close physical association with each other. These are: the antenna chlorophyll complexes associated with PS I and PS II units (known as Chl a_I and Chl a_{II}, respectively) and the light-harvesting Chl a/b-protein complex (LHC_{II} in our terminology) which transfers some energy to PS I but serves largely as antenna to PS II. The interaction of these pigment assemblies can be determined form low-temperature (77 K) fluorescence at 685, 695 and 735 nm. These emission bands arise from LHC_{II}, Chl a_{II} and Chl a_I, respectively [26]. The bipartite model is a simplification of the tripartite model in which the LHC_{II} and Chl a_{II} are regarded as one functional unit. This assumption allows us to rationalize the pigment bed as a two-component system. The models enable us to determine the initial distribution of absorbed quanta within the pigment assemblies as well as the transfer of excitons between these components.

The results presented in Table II clearly demonstrate a reversible effect of phosphorylation on energy transfer from PS II to PS I. The transfer factor $\psi T_{(II \to I)(m)}$ was increased more by phosphorylation than it was by depletion of Mg^{2+}. The phosphorylation of LHC_{II} [20] does not apparently override the Mg^{2+} effect, since $\psi T^{-}_{(II \to I)(m)}$ is greater than $\psi T^{+}_{(II \to I)(m)}$ for phosphorylated membranes. The response is clearly reduced, however, since the effect of Mg^{2+} depletion on

TABLE IV

CALCULATED VALUES OF $\Psi T(3,2) \cdot \Psi T(2,3)$ FOR NONPHOSPHORYLATED, PHOSPHORYLATED AND DEPHOSPHORYLATED MEMBRANES WITH AND WITHOUT $MgCl_2$

Calculations were made with assumed values of $\gamma = 0.5$, $\beta = 0.2$ and $\psi T(2,3)_{(m)} = 0.90$ [11].

	Nonphosphorylated		Phosphorylated		Dephosphorylated	
	+Mg	−Mg	+Mg	−Mg	+Mg	−Mg
$\Psi T(3,2) \cdot \Psi T(2,3)$	0.38	0.30	0.20	0.23	0.34	0.33

TABLE V

VALUES OF F_v/F_0 CALCULATED FROM TABLE I FOR NONPHOSPHORYLATED, PHOSPHORYLATED AND DEPHOSPHORYLATED CHLOROPLAST MEMBRANES

	Nonphosphorylated		Phosphorylated		Dephosphorylated	
	$+MgCl_2$	$-MgCl_2$	$+MgCl_2$	$MgCl_2$	$+MgCl_2$	$-MgCl_2$
F_v^{695}/F_0^{695}	1.6	0.94	0.96	0.69	1.26	0.90

$\psi T_{(II \rightarrow I)(m)}$ is half that (in percentage terms) of the nonphosphorylated membranes. It is worthy of note that the value of $\psi T^{+}_{(II \rightarrow I)(m)}$ for phosphorylated membranes is almost identical to the value of $\psi T^{-}_{(II \rightarrow I)(m)}$ for nonphosphorylated and dephosphorylated membranes. In contrast, the value of α^+ for phosphorylated membranes is significantly greater than α^- of nonphosphorylated and dephosphorylated membranes. In phosphorylated membranes α is not further increased by removal of Mg^{2+}. These observations suggest that Mg^{2+} and membrane phosphorylation have subtly different effects on membrane-energy distribution. The effects on $\psi T_{(II \rightarrow I)(m)}$ appear to be complementary and additive; the action of Mg^{2+} depletion on α is superceded and displaced by the response to membrane phosphorylation. At this point in the discussion it is necessary to distinguish, briefly, the two phenomena $\psi T_{(II \rightarrow I)(m)}$ and α. The former is a measure of the total energy transfer between PS II and PS I, including energy transfer directly from the PS II reaction center and Chl *a* II [13]. This term, sometimes described as spillover, appears to respond to changes in membrane surface charge [7] caused either by cation changes [7] or membrane phosphorylation [23]. The parameter α is the proportion of absorbed quanta going directly to PS I, this value includes quanta absorbed by Chl a_1 and those quanta absorbed by LHC_{II} which are transferred to PS I directly [13]. The first of these contributions to α is presumably a constant, so that increases in α must reflect a change in transfer from LHC_{II}. Therefore, the increase in α is inversely related to the coupling of LHC_{II} to PS II.

Results presented in Table IV confirm that LHC_{II}-PS II coupling $[\Psi T(3,2) \cdot \Psi T(2,3)]$ is reversibly decreased by phosphorylation of LHC_{II}. Although depletion of Mg^{2+} also reduces this coupling, the effect is much smaller than that of phosphorylation. The coupling term $\Psi T(3,2) \cdot \Psi T(2,3)$ of phosphorylated membranes is not further reduced by cation depletion; values of $\Psi T(3,2) \cdot \Psi T(2,3)$ presented in Table IV show exactly the same trends as the α values in Table II. From the data calculated in this paper it is clear that membrane phosphorylation reversibly increases α by reducing the coupling of LHC_{II} to PS II. Previously observed effects of cation depletion on α [13] and on $\Psi T(3,2) \cdot \Psi T(2,3)$ [11] do not appear significant in comparison. Phosphorylation also reversibly stimulates PS II $\rightarrow$ PS I energy transfer; in this case, the Mg^{2+} effect appears to be additive to that of phosphorylation. We interpret these observations as showing that the State 1-State 2 transition phenomenon involves two distinct, but related, mechanisms. It appears that in vivo control of α rests with the state of membrane protein phosphorylation, which is in turn controlled by the oxidoreduction state of carriers between PS II and PS I [5].The value of $\psi T_{(II \rightarrow I)}$, on the other hand, is controlled jointly by ion concentration and membrane phosphorylation, possibly through the membrane surface charge [7,23].

The demonstration of reversible changes in parameters such as α and $\psi T_{(II \rightarrow I)(m)}$ is in itself not proof of real changes in membrane function. Yet, if α and $\psi T^{+}_{(II \rightarrow I)(m)}$ for nonphosphorylated membranes are summed, the total proportion of quanta reaching PS I is only 35%. Upon phosphorylation, α^+ and $\psi T^{+}_{(II \rightarrow I)(m)}$ account for 52% of the total quanta. From discussion of the bipartite and tripartite model systems [22], it is apparent that the determined values of α must be regarded as minimum values. Even so, the change in energy distribution is large enough to induce real changes in membrane function, i.e., a State 1-State 2 transi-

tion. This statement is supported by observations of increases in PS I relative quantum yields upon membrane phosphorylation [28].

From Fig. 3 we are able to determine values of $F^{684}\gamma$ for nonphosphorylated and phosphorylated membranes. The extrapolated value is equal in each case, although the slope of the plot does vary considerably. $F^{684}\gamma$ represents the intensity of fluorescence due to direct excitation of LHC_{II} [13]. This indicates no degradation in the pigment associated with the LHC_{II} protein. This term would not be expected to be altered by LHC_{II}-PS II coupling. The slope of the F_m^{684} vs. F_m^{695} plot is an indication of the $\Psi T(3,2) \cdot \Psi T(2,3)$ term.

The value of $\Psi(3,2) \cdot \Psi T(2,3)$ has been suggested to be an estimate of connectivity between PS II units [24]. Kyle et al. [21] have demonstrated that PS II-PS II energy transfer is reversibly inhibited by phosphorylation of LHC_{II}. They have discussed these results in terms of the 'separate package' and 'matrix' models for the photochemical apparatus and have interpreted their data as support for the 'connected package' theory proposed by Butler [24]. The results determined here from low-temperature fluorescence are totally consistent with the interpretation presented by Kyle et al. [21].

The reversible effect on PS II connectivity, induced by LCH_{II} phosphorylation, demonstrated here and by Kyle et al. [21] contradicts the concept of a rigid structurally heterogeneous population of PS II reaction centers as proposed by Melis and co-workers [25–27]. Kyle et al. [21] have suggested that PS IIα and PS IIβ [25–27] exist only as different states of connectivity between LHC_{II}-PS II units rather than different structures in the membrane. A high degree of connectivity between LHC_{II}-PS II units corresponds to PS IIα [21], reducing this connectivity increases the PS IIβ population [21,24].

In a recent publication, Butler [24] has equated the theories proposed by Melis and co-workers [25–27] with his own photosynthetic models. Butler suggests that F_v^{695}/F_0^{695} is a measure of the proportion of PS IIα/PS IIβ (the degree of connective packaging), and that F_v^{695}/F_0^{695} would be higher for the PS IIα component. For a matrix model system (analogous to PS IIα) he predicts a F_v^{695}/F_0^{695} ratio of 1.5. Table V shows values of F_v^{695}/F_0^{695} calculated from the data of Table I (similar results were obtained using the data of Table III). In nonphosphorylated membranes in the presence of $MgCl_2$ (where connectivity is highest) the F_v^{695}/F_0^{695} ratio is 1.6, for phosphorylated membranes (where connectivity is lowest) the value falls to 0.69. We interpret these data as further support for the concept that the photosynthetic apparatus exists as a connected package model. The connection between these packages is clearly reversibly affected by phosphorylation of LHC_{II}.

Conclusion

Using data from low-temperature (77 K) fluorescence induction transients, we have demonstrated the physiological role of protein phosphorylation in photosynthesis. Phosphorylation of LHC_{II} increases α by reducing the coupling of LHC_{II} to PS II $[\Psi T(3,2) \cdot \Psi T(2,3)]$. At the same time, the value of $\psi T_{(II \to I)}$ (spillover) is increased by phosphorylation. Both of these effects are reversible upon dephosphorylation of the membranes. Comparison of the phosphorylation effects with those induced by Mg^{2+} depletion allow us to make two important statements. The in vivo control of α [and $\Psi T(3,2) \cdot \Psi T(2,3)$] lies with membrane phosphorylation, which is in turn controlled by the oxidoreduction state of electron carriers. Control of $\psi T_{(II \to I)}$ is also under protein phosphorylation control and is further influenced by cation concentrations.

The demonstration of reversible changes in LHC_{II}-PS II energy/coupling (and by implication PS II-PS II transfer) gives support to the connected package model. This observation is in contradiction to proposed structurally heterogeneous populations of PS II centers.

Acknowledgements

Supported in part by NSF Grant No PCM-8023031. D.J.K. is recipient of a Natural Sciences and Research Council of Canada Fellowship.

References

1 Bonaventura, C. and Myers, J. (1969) Biochim. Biophys. Acta 189, 366–386

2 Murata, N. (1969) Biochim. Biophys. Acta 172, 242–257
3 Williams, W.P. (1977) in Primary Processes in Photosynthesis (Barber, J., ed.), pp. 99–147, Elsevier, Amsterdam
4 Ried, A. and Reinhardt, B. (1980) Biochim. Biophys. Acta 592, 76–86
5 Allen, J.F., Bennett, J., Steinback, K.E. and Arntzen, C.J. (1981) Nature 291, 25–29
6 Vernotte, C., Briantais, J.M., Armond, P. and Arntzen, C.J. (1975) Plant Sci. Lett. 4, 115–123
7 Barber, J. (1980) FEBS Lett. 118, 1–10
8 Chow, W.S., Ford, R.C. and Barber, C.J. (1981) Biochim. Biophys. Acta 635, 317–326
9 Satoh, K., Strasser, R.J. and Butler, W.L. (1976) Biochim. Biophys. Acta 440, 337–345
10 Butler, W.L. and Strasser, R.J. (1977) Proc. Natl. Acad. Sci. U.S.A. 74, 3382–3385
11 Butler, W.L. and Strasser, R.J. (1977) Proceedings of the 4th International Congress on Photosynthesis (Hall, D.O., Coombs, J. and Goodwin, T.W. eds.), pp. 11–20, The Biochemical Society, London
12 Butler, W.L. (1979) Chlorophyll Organization and Energy Transfer in Photosynthesis, Ciba Found. Symp. 61 (New Series), pp. 237–252, Excerpta Medica, Amsterdam
13 Butler, W.L. and Kitajima, M. (1975) Biochim. Biophys. Acta 396, 72–85
14 Steinback, K.E., Burke, J.J. and Arntzen, C.J. (1979) Arch. Biochem. Biophys. 195, 546–557
15 Steinback, K.E., Burke, J.J., Mullet, J.E. and Arntzen, C.J. (1978) in Chloroplast Development (Akoyunoglou, G. and Argyroudi-Akoyunoglou, J.M., eds.), pp. 389–400, Elsevier, Amsterdam
16 Burke, J.J., Ditto, C.L. and Arntzen, C.J. (1978) Arch. Biochem. Biophys. 187, 252–263
17 Bennett, J. (1977) Nature 269, 344–346
18 Bennett, J. (1979) Eur. J. Biochem. 99, 133–137
19 Bennett, J. (1980) Eur. J. Biochem. 104, 85–89
20 Bennett, J., Steinback, K.E. and Arntzen, C.J. (1980) Proc. Natl. Acad. Sci. U.S.A. 77, 5253–5257
21 Kyle, D.J., Haworth, P. and Arntzen, C.J. (1982) Biochim. Biophys. Acta 680,
22 Butler, W.L. (1977) in Encyclopedia of Plant Physiology, New Series, Vol. 5 (Trebst, A. and Auron, M., eds.), pp. 149–167, Springer-Verlag, Berlin
23 Kyle, D.J., Bose, S., Steinback, K.E., Watson, J. and Arntzen, C.J. (1981) Plant Physiol. 67, S-34
24 Butler, W.L. (1980) Proc. Natl. Acad. Sci. U.S.A. 77, 4697–4701
25 Melis, A. and Schreiber, U. (1979) Biochim. Biophys. Acta 547, 47–57
26 Melis, A. and Homann, P.H. (1976) Photochem. Photobiol. 23, 345–350
27 Melis, A. (1978) FEBS Lett. 95, 202–206
28 Steinback, K.E., Bose, S. and Kyle, D.J. (1982) Arch. Biochem. Biophys., in the press